Simulation analysis on fatigue damage mechanism and life assessment of rigid catenary pillar of railway lines

Wei Du
China Academy of Railway Sciences Corporation Limited, Metals and Chemistry Research Institute, Beijing, China
Suxia Zhou
School of Mechanical and Electrical Engineering and Vehicle Engineering, Beijing Jianzhu University, Beijing, China, and
Zhongyu Yi, Ruohan Xiang, Yishuo Liu, Zhenping Shi and Shanqing Peng
China Academy of Railway Sciences Corporation Limited, Metals and Chemistry Research Institute, Beijing, China

Received 6 January 2025
Revised 3 March 2025
Accepted 13 March 2025

Abstract

Purpose – As a key structure in the railway power supply system, the overhead catenary pillar carries the entire weight and dynamic load of the contact suspension device and supporting equipment. Its stability and reliability are directly related to the operational safety and efficiency of electrified railways.

Design/methodology/approach – Regarding the phenomenon of abnormal shedding of coating above the support under the cantilever of the catenary pillar in the track running line, a three-dimensional model is established to analyse the rigid cantilever type catenary and the force analysis of the cantilever part is carried out by using ABAQUS to calculate the contact force of the bow network under different running speeds of the high-speed train. The load is applied at the locator end of the simplified model of the cantilever to get the support reaction force at the connection between the cantilever and the support.

Findings – The support reaction force is applied as a load to the three-dimensional model of the pillar support; the stress cloud and the stress extreme value of 86.14 MPa are obtained for the pillar and the support part and the fatigue life of the pillar's key parts is calculated to be 12.02 years, respectively.

Originality/value – The upper part of the lower support of the high-speed rail catenary pillar is subjected to the alternating load transmitted by the bow net, which causes the fretting damage at this position, resulting in the abnormal peeling of the coating on the upper part of the lower support. Through combining the ABAQUS analysis with the structural characteristics and operating conditions of the catenary system, the main causes of component failure are determined.

Keywords Catenary, Fretting damage, ABAQUS, Coating

Paper type Research paper

1. Introduction

With the rapid development of high-speed railways, the requirements for safe operation of catenary for high-speed railways are getting higher. As the main content of modern railway construction, catenary is the key component of electrified railway, which mainly undertakes the mission of providing reliable electric power to rolling stock and electric locomotives. In recent years, with the increased proportion of electrified railways in China's railway mileage,

Supported by the State Railway Administration of China (J2022G008).

Railway Sciences
Vol. 4 No. 3, 2025
pp. 337-355
Emerald Publishing Limited
e-ISSN: 2755-0915
p-ISSN: 2755-0907
DOI 10.1108/RS-01-2025-0001

harsh environment supply system not only faces the rapid development of new technologies, new equipment and new materials and faces the continuous improvement of power supply operation levels but also the hostile conditions of power supply equipment in external environments and many other troubles.

The catenary system is one of the main power supply systems in modern high-speed railways, which is the source of power for high-speed train operation. The traction power of high-speed EMU is obtained through the traction power supply system composed of a traction substation and catenary. A traction substation converts the three-phase high-voltage power supply delivered by the power system into an AC 27.5 kV single-phase power supply for the catenary power supply. The catenary system consists of support devices, contact suspension, positioning devices, pillars and foundations, etc. The support devices include cantilevers, horizontal tie rods, suspended insulator strings, bar insulators and other special support equipment. The contact suspension consists of contact wires, suspension strings, bearing cables, compensators, etc. including various fastening bolts, and its parts and components amount to hundreds of kinds. It is a special form of transmission line erected over the railway line to provide electricity to the electric locomotive. Besides, there is no spare line in its service process, and it needs to withstand the complex and severe environment, which is a great test of the catenary – not only the test of the harsh environment but also the test of pantograph impact vibration. Once damaged, it will interrupt the traffic, which will affect the national economic interests, people's lives and property safety. Therefore, the safety and reliability of the catenary are extremely important, as shown in Figure 1.

The catenary pillars bear the load of contact suspension and support equipment, which are used to realise the power supply to electric locomotives and directly affect the operational safety of the railway. The dynamic performance of the pantograph–catenary determines the reliability of power transmission and the quality of power supply. The catenary has the

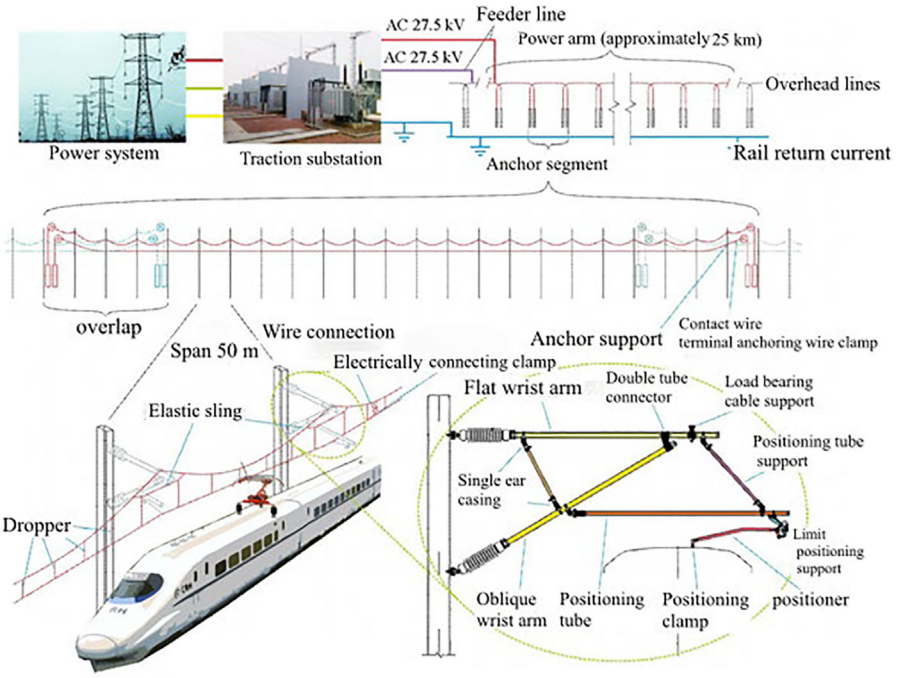

Figure 1. High-speed railway catenary system. **Source(s):** Authors' own work

characteristics of a large span and high flexibility and is very sensitive to the disturbance of external loads. Under the action of external loads (wind load, ice cover, lifting force of pantograph, etc.), a vibration phenomenon will occur in the catenary. Excessive vibration will lead to damage and deterioration of the current receiving performance of the support system of the pantograph–catenary system due to fretting deformation, which is more likely to cause problems such as fatigue of the catenary system, disconnection of the pantograph or even pantograph scratch accident in serious cases. The cantilever is the support device of the catenary, which plays the role of supporting and positioning the catenary and bears the electrical and mechanical loads. The environmental loads borne by the contact wire and bearing cable will be transferred to the cantilever, which will easily cause fatigue and damage of the cantilever.

The catenary is subjected to long-term and frequent mechanical vibration in service, but the form of its load is very complex due to the fact that the high-speed catenary components bear a variety of local alternating loads such as tensile, compressive, shear and torsion. At the same time, the catenary components in service are also affected by many environmental and operating factors, such as time-varying high current, wind vibration, temperature difference, corrosion, wind and sand, rain, snow, frost and fog (Chang, 2013; Liu, Song, & Liu, 2015a; Wang, 2009; Xue & Du, 2022; Zhang, Li, Ma, & Li, 2023; Cheng *et al*., 2024). Causes of catenary component fatigue load can be further subdivided into wind vibration, over-bow impact, self-excited vibration, hot and cold stress, etc. The corrosive environment can also be divided into environmental pollution, electrochemical corrosion and stress corrosion. It can be seen that the service environment of catenary component is very complex, which is determined by mechanical fatigue load, corrosion, cold and hot stress, high current, ice, environmental pollution and other factors, and there are a lot of reasons that can result in a complex service environment (such as the flexible structural characteristics of the catenary itself, the sliding current of pantograph, etc.). The stress load, environmental corrosion and high current in the service environment of the catenary components have a greater impact on the service life of the components, and there are fewer related studies on the catenary components at present. Some scholars such as Ngamkhanong, Kaewunruen and Pombo have conducted research on stress loads, environmental corrosion and other aspects of catenary components in China using methods including theoretical derivation, finite element analysis, experimental simulation, etc. (Haiderali, 2020; Sakdirat & Tao, 2019; Sakdirat, Chayut, & Lichen, 2021).

There are numerous cases of component failures caused by catenary failures and further lead to accidents in high-speed railways. The catenary operating in the open air is subject to a wide range of operating conditions. Both pantograph impacts and random environmental loads will affect the safe and reliable operation of high-speed railways. The cantilever structure is used as a support device for the catenary, which supports and positions the catenary and bears the electrical and mechanical loads. The vibration excitation and environmental loads borne by the contact wire and the carrier cables will be transferred to the cantilever, which will easily cause the fatigue and destruction of the cantilever. The stability of the cantilever structure has a great influence on the quality of the pantograph–catenary current collection. In this paper, through the establishment of a finite element model of the cantilever and the analysis of the static and dynamic mechanical properties of the cantilever, the stress–strain cloud diagrams of the cantilever under different working conditions are obtained, and the load transfer law between each rod of the cantilever is deduced. The correctness of the finite element model of the arm is verified by the bench test of the cantilever. The results of the study provide a certain theoretical basis for the optimal design of the cantilever structure and the development of a new type of higher-speed cantilever system and also provide ideas for the detection of faults in the key parts of the cantilever system, which have a certain degree of practical significance in engineering. The research of catenary abnormality mainly includes the fatigue life of catenary, the quality of pantograph-catenary current collection, fatigue life prediction and other issues (Cao, Ke, Deng, & Liu, 2010; Wang, Deng, Li, Tian, & Ke, 2005). At present, the catenary faults operating in China's rail transit mainly include electrical burn faults, external influence

faults and mechanical structure faults. In the form of achieving reliable distribution between components, it can improve the safety and reliability of the catenary.

The research of catenary has been carried out for decades. Japanese scholars Noburo Ehara *et al.* established a universal model of pantograph unary and binary mass blocks, the calculation of which discretises the carrier cable and contact line as a point of concentrated mass and the suspension string is equivalent to a rigid rod. However, the bending and tensile stiffness of the carrier cable and the contact line are not considered in the model of literature (Wang *et al.*, 2005). German scholars M. Link and G. Diana used a finite element model to analyse and calculate the dynamic characteristics of the pantograph–catenary with their common force. The intrinsic frequency of the catenary is calculated, and each single frequency is superimposed to obtain the response of the catenary (Diana, Bruni, Collina, & Fossati, 1998; Liu, Yong, & Guo, 2015b; Vinayag, 1983). Zhang Weihua and his team established a mathematical model of the catenary and studied the dynamics of the pantograph–catenary system through the modal superposition method. Under his influence, many scholars in China adopted the finite element method to establish the finite element model of the catenary (Link, 1981; Link & Nowak, 1987; Wu, 1996; Zhang & Shen, 1991).

The cantilever device is the main support component in the support device, and its main components consist of the flat/oblique cantilever, the cantilever base and the cantilever support, as shown in Figure 2. For these components, the main failure states include fracture, bending, burn, deviation and damage. As shown in Table 1, these components are categorised into normal and severe according to their severity, and the causes of each type of failure are explained.

In the catenary support system of a high-speed railway, the pillar is a device that connects the ground with the cantilever system and the pillar and the cantilever system are mainly connected by bolts. The catenary pillar plays the role of support and force in the whole set of catenary support system and the organic coating on the outer side of the pillar is a polyurethane coating with a thickness of about 0.08–0.1 mm. As shown in Figure 3, the position marked out by the red circle has an obvious coating shedding. Coating shedding is caused by the penetration of water and corrosive media through the coating, resulting in osmotic pressure between the coating and the substrate and the formation of a concentration gradient, leading to electrochemical reactions. The interior of the coating gradually begins to corrode and corrosion products grow in the inner layer, usually forming bubbles. In the case of coating cracking under stress, corrosion products will grow along the crack.

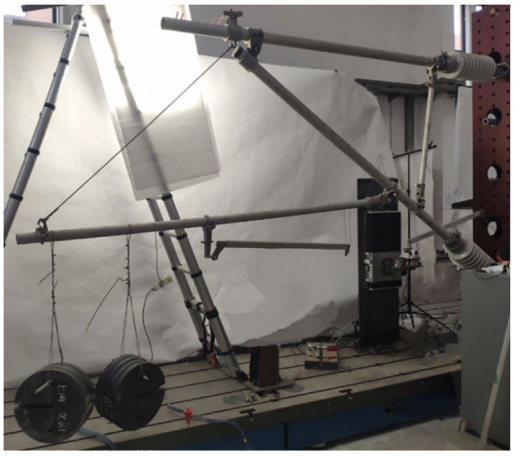

Figure 2. Cantilever device. **Source(s):** Authors' own work

Table 1. Failures states of the cantilever device

Component	Degree of failure	Fault state	Rationale
Flat/oblique cantilever	Normal	Bending	Pantograph failure and accident
		Deviation	Carrier cable breakage
	Severe	Fracture	Pantograph failure and accident
		Burn	Foreign object lap
Cantilever base	Normal	Bolt looseness	Accidents such as fatigue, poor material, corrosion, theft of nuts and threading nails, etc
	Severe	Fracture	Design and installation defects and long-term fatigue
Cantilever support	Normal	Damage	Accidents such as flying birds
	Severe	Fracture	Pantograph injuries, etc

Source(s): Authors' own work

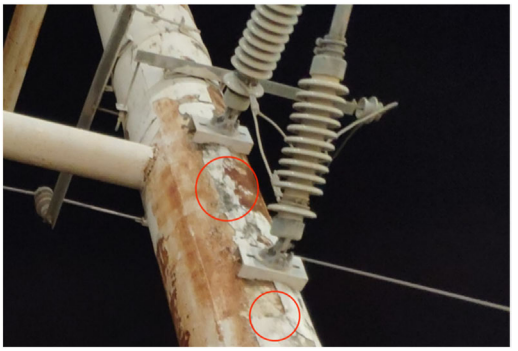

Figure 3. Shedding of surface coating on pillar device. **Source(s):** Authors' own work

The connecting components of the supporting device mainly include the double ears of the sleeve, the clamp of the supporting tube, the support cable support and the iron cover pressure cap. The main fault states include fracture, detachment, deformation, looseness, etc. According to the severity of the components, they are divided into two types: general and severe, as shown in Table 2.

Table 2. Connection components of supporting device

Component	Degree of failure	Fault state	Rationale
Double ear casing	General	Deformation	Poor stress
		Loosen	Natural factors
	Serious	Fracture	Corrosion and poor stress
Bearing cable base	General	Iron cap pressure cap fracture	Smash off accident
	Serious	Loose load-bearing cable support	U-shaped ring fracture
Support pipe clamp	General	Loosen	Loose bolts, excessive opening of β pin, fracture of opening pin (fatigue) and pin detachment
	Serious	Fall off	Loose bolts, fatigue and pantograph malfunction

Source(s): Authors' own work

2. Materials and methods

The traditional aluminium alloy cantilever structure has many components, fasteners and various forms and the catenary cantilever and positioning device adopt a straight limit positioner + flexible suspension positioning tube, combined carrier cable seat, combined positioning ring and other parts. Referring to the OCS technical conditions requirements (Chen, 2016; Li, 2017; Luo, Mo, Han, Yan, & Zhang, 2018a; Harak, Sharma, & Harsha, 2015; Ministry of Railways, Department of Science and Technology, 2009) for the loading of the cantilever structure, the specific loading mode is as follows: horizontal load F1 and vertical load F2 are applied at the carrier cable seat and horizontal load F3 and vertical load F4 are applied at the position of the locator line clamp. The traditional cantilever structure device and its specific loading situation are shown in Figure 4.

The finite element model of the catenary structure is established in ABAQUS finite element calculation software, and the catenary structure model is divided into 76,168 units and 96,072 nodes. The material properties of the pillar are set according to Q235 structural steel, whose modulus of elasticity E = 210,000 MPa, Poisson's ratio is 0.3 and the mass density is 7,850 kg/m^3. The material properties of the cantilever structure are set according to T6 aluminium alloy, whose modulus of elasticity E = 700,000 MPa, Poisson's ratio is 0.3 and the mass density is 2,700 kg/m^3. The partial modelling of the overall structure of the catenary is shown in Figure 5.

3. Results and discussion

Due to the excessive contact surfaces in the cantilever structural model, in order to reduce the simulation computing time and lower the calculation amount to the actual feasible range, the cantilever can be replaced by using the tube unit, and the force analysis and simplification of the overall model will be conducted. The calculation will be carried out by simplifying the three-dimensional model loading for obtaining its stresses and support reaction forces and using the support reaction forces to calculate the actual three-dimensional model stresses and strains; then the fatigue life of the pillar overall model can be further calculated.

3.1 Establishment of three working conditions

According to the dynamic performance index of catenary–pantograph interaction in the TB10009-2016 Code for Design of Railway Traction Power Supply, three conditions of ordinary, medium and high speed are selected for analysis, respectively, corresponding to 120 km/h, 160 km/h and 300 km/h each, in which the 120 km/h and the force of the gravitational cable are determined in accordance with the standard of OSC (Luo, Lu, Yan, & Zhang, 2018b; Xu, 2014; Vingsbo & Söderberg, 1988). The contact forces for the two

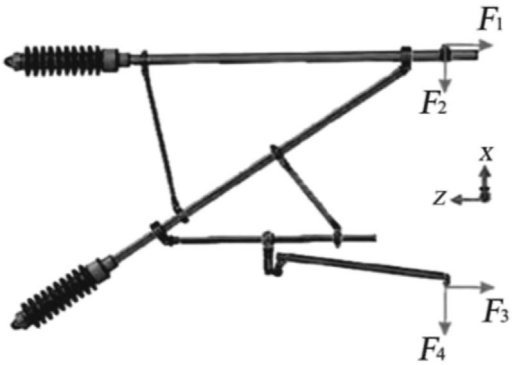

Figure 4. Load application position of cantilever structure. **Source(s):** Authors' own work

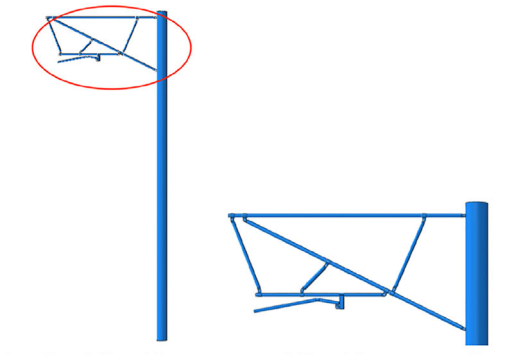

Figure 5. Overall modelling of the catenary and structural modelling of the cantilever. **Source(s):** Authors' own work

operating speeds at 160 km/h and 300 km/h are calculated according to the dynamic performance index of the catenary–pantograph interaction, as shown in Table 3.

The maximum average contact force of pantograph–catenary is calculated according to the standard at medium speed to calculate its fatigue life, and the contact force amplitude at high speed is selected as the limit working condition. Due to the work of the support, it can still have the performance of structural stability (Jin & Mall, 2004; Nakazawa, Sumita, & Maruyama, 1992; Naidu & Raman, 2005), a flexible swing and other properties under 1.5 times its maximum working load and the typical installation of a cantilever support structure, the 1.5 times the force is selected as the limit working condition:

Maximum contact force of the pantograph–catenary at operating speed of 300 km/h:

$$\left(0.00097 \times 300^2 + 70\right) \times 1.35 \times 1.5 = 318.525$$

The average contact force of the pantograph–catenary at an operating speed of 160km/h:

$$\left(0.00047 \times 160^2 + 90\right) = 102.032$$

Table 3. Dynamic performance indexes of catenary–pantograph interaction

Design speed v (km/h)	160	200	250	300	350
Average contact force fm(N)	$F_m \leq 0.000\,47v^2 + 90$		$F_m \leq 0.000\,97v^2 + 70$		
Maximum contact force fmax(N)	300		350		
Minimum contact force fmin(N)	0		0		
Maximum standard deviation of contact force ρmax(N)	0.35*fm*				

Source(s): Authors' own work

According to the relevant standards, the load combinations corresponding to the three speeds are derived and the operating speeds corresponding to the three working conditions are 300km/h, 160km/h and 120km/h. The load combinations are shown in Table 4.

Literature (Lykins, Mall, & Jain, 2001; Poon & Hoeppner, 1979; Tan *et al.*, 2018) used a pantograph system model with three degree of freedom to linearise it according to the coupled dynamic equations of the pantograph-catenary, and simulation calculations for different speeds were carried out, resulting in the cyclic period of the pantograph–catenary contact load at different speeds is 1 s, The model was loaded with the above load combinations in order to calculate the fatigue life of the catenary under the ultimate working condition.

3.2 Dynamic simulation analysis of simplified cantilever structure

Based on the three working conditions, the strain and stress in the cantilever system are calculated. According to the force of the catenary at different speeds, the vertical and horizontal loads are applied to the carrier cables of the catenary cantilever system and the position of the contact line, respectively, and the corresponding calculation results are shown in Figures 6 and 7, respectively.

As it can be seen in Figure 6, the maximum strain of the cantilever structure under different working conditions is at the end of the positioner. The maximum values of the strains in working conditions 1–3 are 3.9 mm, 12.24 mm and 25.34 mm, respectively, and the strains in the rest of the cantilever structure are so small that they can be almost neglected.

As it can be seen from Figure 7, the maximum stress of the catenary cantilever structure occurs at the limit locator support in working conditions 1 and 2, with maximum values of 133.2 MPa and 61.95 MPa, respectively, while in working condition 3, the maximum stress in the catenary cantilever structure is 28.27 MPa, which occurs at the position of the double casing connection. In addition, the stress concentration will be generated at the structure connection position (such as the connection position of cantilever support and flat cantilever).

3.3 Analysis of support reaction forces

According to the simulation results of the simplified cantilever structure model in ABAQUS, the support reaction force of the simplified cantilever structure model of the catenary under three speeds corresponding to working conditions was extracted and the change of the support reaction force in 1 s was obtained. RF1, RF2 and RF3 are the lateral, vertical and longitudinal support reaction force, respectively, and the support reaction force at the connection between the cantilever and the support is shown in Figure 8.

It can be seen through the support reaction force of the cantilever of the catenary in three working conditions that the corresponding support reaction forces under different working conditions have the same trend of change, and all of them oscillate around a certain value after 0.4 s. The maximum value of the support reaction force in working condition 2 and 3 occurs around 0.8 s, while the maximum value of the working condition 1 occurs at 1 s, as shown in Figure 9.

Table 4. Working load of cantilever structure

Load type	Perpendicular to the carrier cable	Horizontal to the carrier cable	Perpendicular to the contact line	Horizontal to the contact line
Working condition 1: maximum load	4,000 N	2,000 N	318 N	2,500 N
Working condition 2: average load	1,905 N	1,064 N	102 N	1,074 N
Working condition 3: normal load	1,150 N	355 N	30 N	357 N

Source(s): Authors' own work

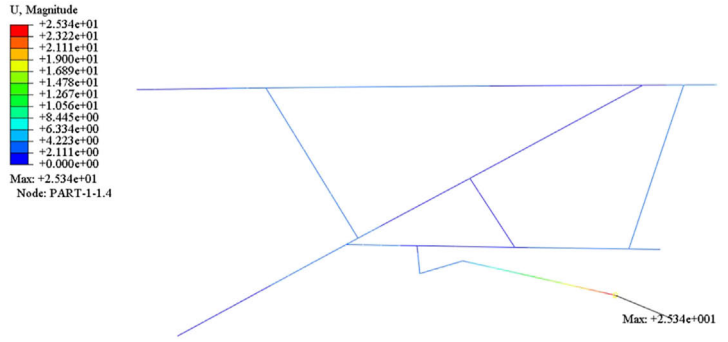

Strain nephogram of simplified structural model in working condition 1

(a)

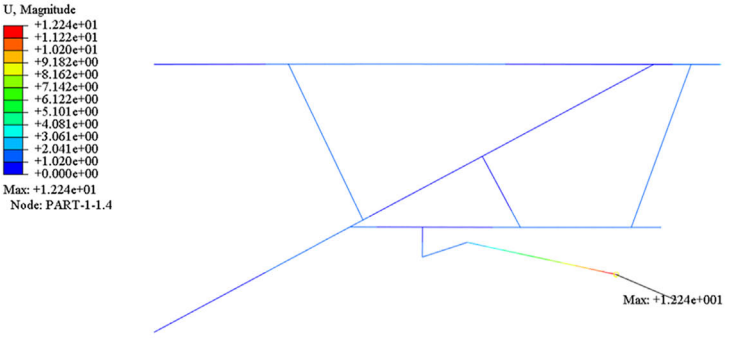

Strain nephogram of simplified structural model in working condition 2

(b)

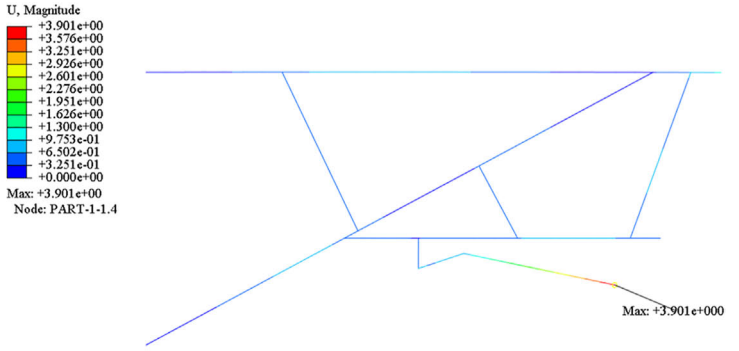

Strain nephogram of simplified structural model in working condition 3

(c)

Figure 6. Strain nephogram of catenary cantilever structure in three working conditions. **Source(s):** Authors' own work

3.4 Dynamic simulation analysis of branch catenary pillar model

The support reaction force obtained from the simplified model of the cantilever structure under three working conditions is applied to the connection of support and cantilever of the catenary pillar model, and the strain and stress distribution at the pillar and cantilever support under the corresponding working conditions are calculated, and the results are shown in Figure 10–13.

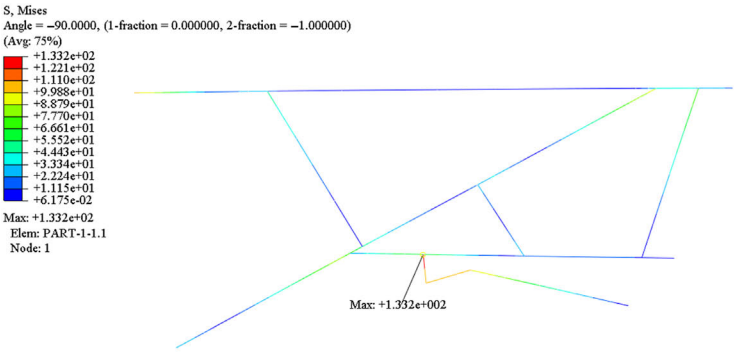

Stress of simplified cantilever structural model in working condition 1

(a)

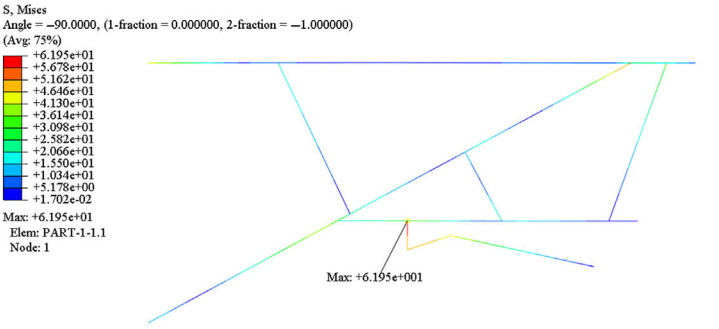

Stress of simplified cantilever structural model in working condition 2

(b)

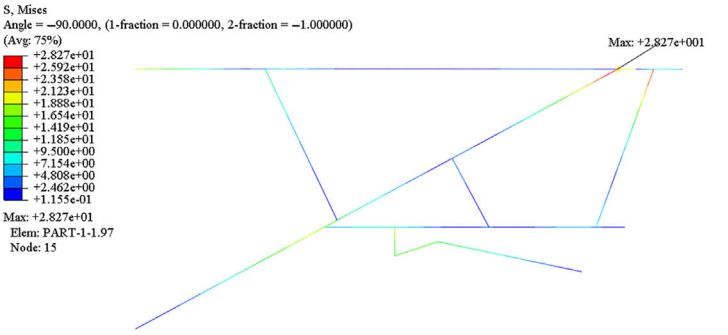

Stress of simplified cantilever structural model in working condition 3

(c)

Figure 7. Stress distribution of catenary cantilever structure for three working conditions. **Source(s):** Authors' own work

Comparing the strain nephogram of the three-dimensional catenary pillar model under three working conditions, it can be obtained that the strain between the two supports is more obvious, the strain below the lower support is relatively small and the overall trend is decreasing from top to bottom. Under different working conditions, the maximum value of strain is at the uppermost part of the pillar and the maximum strain under working condition 1

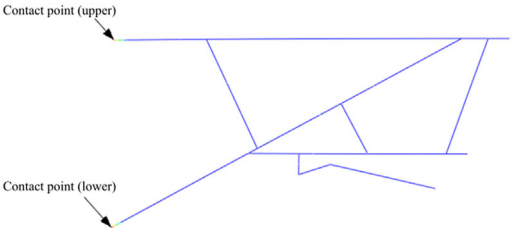

Figure 8. Schematic diagram of the contact points between the pillar and the cantilever structure. **Source(s):** Authors' own work

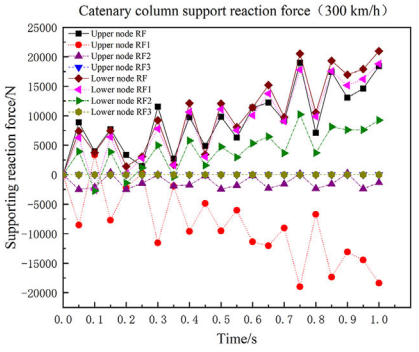

Support reaction forces of simplified cantilever structural model in working condition 1

(a)

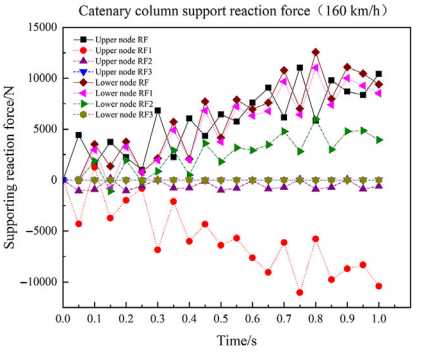

Support reaction forces of simplified cantilever structural model in working condition 2

(b)

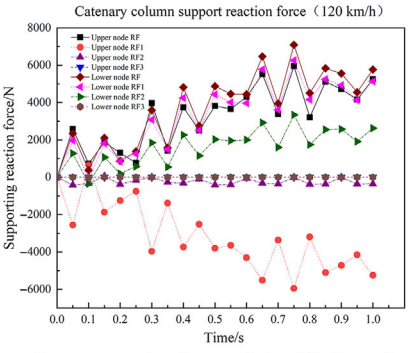

Support reaction forces of simplified cantilever structural model in working condition 3

(c)

Figure 9. Support reaction force of catenary cantilever in three working conditions. **Source(s):** Authors' own work

is 4.552 mm, the maximum strain under working condition 2 is 2.527 mm and the maximum strain under working condition 3 is 0.572 mm.

These figures show that the maximum stress of the pillar cantilever support under the three working conditions all appear in the position of the connection between the pillar and the lower

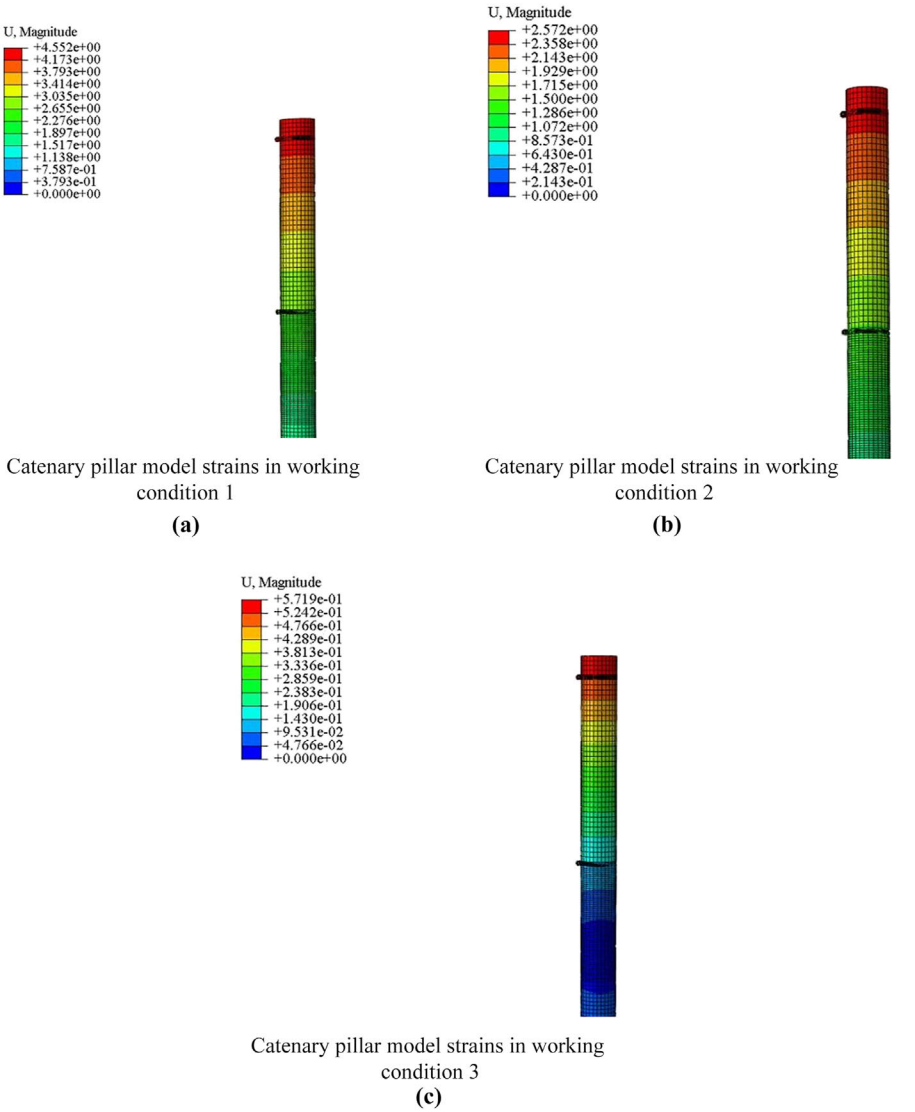

Figure 10. Strain of catenary pillar in three working conditions. **Source(s):** Authors' own work

support, the local stress level in the region is relatively larger, and there is a certain situation of stress concentration around the root of the support. The maximum stress in working condition 1 is 86.14 MPa, the maximum stress in working condition 2 is 51.81 MPa and the maximum stress in working condition 3 is 44.99 MPa.

3.5 Abnormal damage analysis of catenary columns for high-speed train

Through the stress and strain of the catenary pillar model, it can be clearly observed that there are stresses and slight strains above the support under the pillar cantilever, the maximum strain is above the pillar, and it gradually decreases along the vertical direction downward. Stresses under the

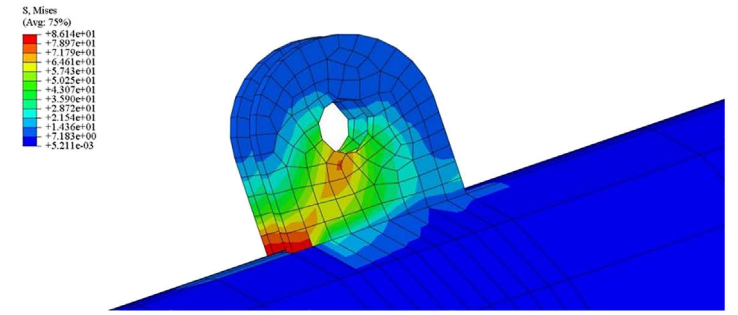

Stress distribution of the support under the catenary pillar model in working condition 1

(a)

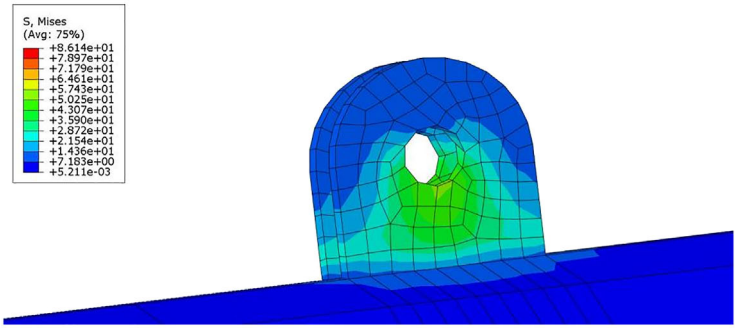

Stress distribution of the support on the catenary pillar model in working condition 1

(b)

Figure 11. Stress distribution of catenary pillar model in working condition 1. **Source(s):** Authors' own work

support of the cantilever will be relatively large in comparison to the other parts, and this region and the other regions have formed an obvious stress junction. Combined with the conclusion of the fretting damage, in the open natural environment, this region is exposed to alternating stress for a long period of time, which can easily lead to the occurrence of fretting damage.

As shown in Figure 14, the red circle position is above the root of the lower support, and the stress is obviously higher than in the other parts of the pillar. In the complex environment, under the influence of weather, humidity, airflow and rainfall, fretting damage occurs at the corresponding position, which is actually manifested as the peeling off of the surface protective coating above the root of the lower support of the cantilever. The magnitude of the strain it receives is not sufficient to lead to the peeling off of the surface coating through the simulation calculation, but the alternating load and open natural environment meet the conditions for the formation of fretting damage, which proves that the coating peeling off at the red circle in Figure 14 is caused by fretting damage.

3.6 Life prediction of catenary pillar

Based on the stresses obtained from the three speeds corresponding to the working conditions, the life prediction calculations of the catenary pillars and the critical parts of the pillars are carried out for each of the three working conditions.

3.6.1 Fatigue life estimation of catenary pillars and pillar critical parts. From the Mises nephogram, it can be seen that the maximum stress of 300 km/h locating support is 133.32 MPa in

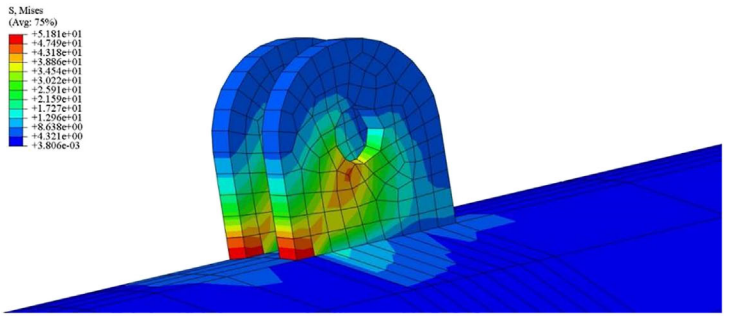

Stress distribution of the support under the catenary pillar model in working condition 2

(a)

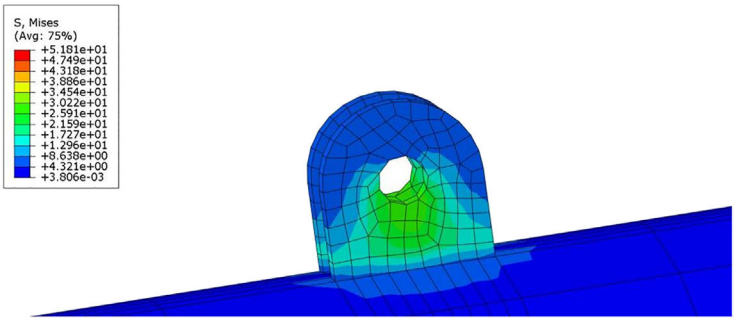

Stress distribution of the support on the catenary pillar model in working condition 2

(b)

Figure 12. Stress distribution of catenary pillar model in working condition 2. **Source(s):** Authors' own work

the pillar critical part of working condition 1, and the minimum stress is 0.1 Mpa; the maximum stress of 160 km/h locating support in working condition 2 is 61.95 MPa and the minimum stress is 0.1 MPa; the maximum stress of 120 km/h locating support in working condition 3 is 28.27 MPa and the minimum stress is 0.1 Mpa. It can be known according to the stress fatigue theory:

Cyclic stress amplitude and average stress calculation:

$$S_a = (S_{max} - S_{min})/2$$

$$S_m = (S_{max} + S_{min})/2$$

Prediction of the basic S–N curve:

Finding the relevant parameters of the material, it can be seen that the damage limit S_u of Q235 is 235 MPa. If the basic S–N curve is expressed by the functional equation $S^m \cdot N = C$, then:

$$m = 3/lg^{(0.9/k)}$$

$$C = (0.9S_u)^m \times 10^3$$

Equal-life conversion:

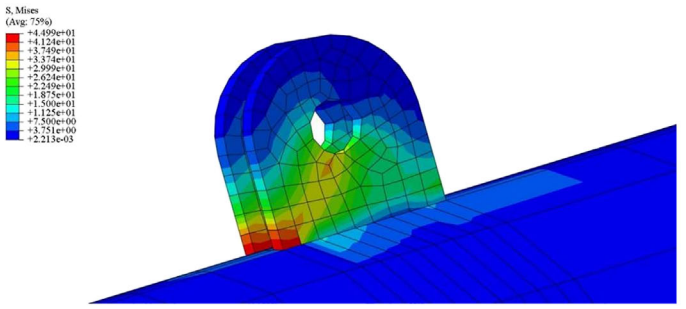

Stress distribution of pillar under the catenary pillar model in working condition 3

(a)

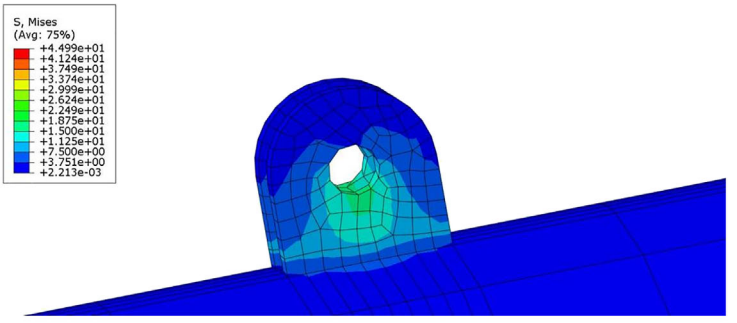

Stress distribution of the support on the catenary pillar model in working condition 3

(b)

Figure 13. Stress distribution of the catenary pillar model in working condition 3. **Source(s):** Authors' own work

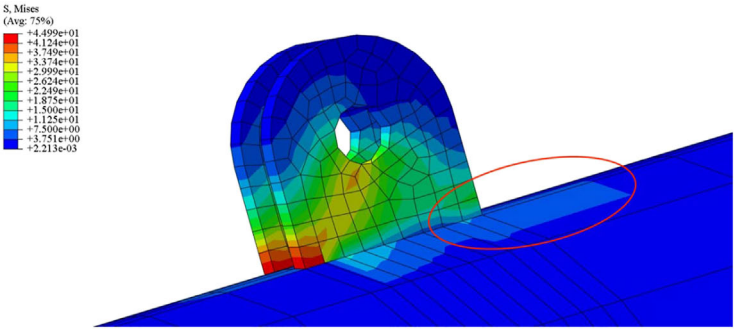

Figure 14. Stress distribution above the lower support of the catenary pillar. **Source(s):** Authors' own work

In order to estimate the fatigue life using the basic S–N curve, it is necessary to convert the actual working cycle stress level equal-life to the stress level under symmetric cycling (R = −1, Sm = 0), which is solved by Goodman's equation $S_{a(R=-1)}$:

$$(S_a/S_{a(R=-1)}) + (S_m/S_u) = 1$$

Life expectancy estimation:

The life under symmetric cycling conditions can be based on the basic S–N curves. The life of the critical connection point of the pillar under maximum stress conditions is assessed as 2.81×107 in working condition 1, 1.31×107 in working condition 2 and 5.97×106 in working condition 3.

$$N = C/S^m$$

After calculating, the life of the pillar critical connection under the maximum stress condition is 2.81×107. In this paper, based on the calculation of 400 trains running every day, 16 cars are grouped into one group and a single car passes through one cycle, so the final life of the discounted life is 12.02 years, much lower than the designed service life of 20–25 years, in line with the results of the literature (Xun *et al.*, 2020; Wang, 2023).

$$B = N/365 \times 400 \times 16 = 12.02$$

3.6.2 Prediction of wrist arm structure lifespan. Part of the positioning hooks and brackets on the high-speed railway line experienced severe wear and tear after less than three years of use, resulting in the replacement of the positioning brackets and the entire locator, as shown in Figure 15. The wear problem of positioning hooks and positioning supports has become a key issue restricting the service life of catenary positioning devices.

For the catenary positioning hook connection node, from the Mises nephogram, it can be seen that the maximum stress of 300 km/h locating support is 356.19 MPa in the positioning hook part of working condition 1, and the minimum stress is 0.1 Mpa; the maximum stress of 160 km/h locating support in the working condition 2 is 51.81 MPa, and the minimum stress is 0.1 MPa; the maximum stress of 120 km/h locating support in the working condition 3 is 44.99 MPa and the minimum stress is 0.1 Mpa. It can be known according to the stress fatigue theory:

Cyclic stress amplitude and average stress calculation:

$$S_a = (S_{max} - S_{min})/2$$

$$S_m = (S_{max} + S_{min})/2$$

Prediction of the basic S–N curve:

Finding the relevant parameters of the material, it can be seen that the damage limit S_u of T6 is 340 MPa. If the basic S–N curve is expressed by the functional equation $S^m \cdot N = C$, then:

$$m = 3/lg^{(0.9/k)}$$

$$C = (0.9S_u)^m \times 10^3$$

Equal-life conversion:

Figure 15. Wear and failure of positioning hook. **Source(s):** Authors' own work

In order to estimate the fatigue life using the basic S–N curve, it is necessary to convert the actual working cycle stress level equal-life to the stress level under symmetric cycling (R = −1, Sm = 0), which is solved by Goodman's equation $S_{a(R=-1)}$:

$$(S_a/S_{a(R=-1)}) + (S_m/S_u) = 1$$

Life expectancy estimation:

The life under symmetric cycling conditions can be based on the basic S–N curves. The life of the critical connection point of the pillar under maximum stress conditions is assessed as 5.17×10^7 in working condition 1, 7.25×10^6 in working condition 2, and 5.64×10^6 in working condition 3.

$$N = C/S^m$$

$$B = N/365 \times 400 \times 16 = 22.14$$

After calculation, the lifespan of the key connection points of the pillar under the maximum stress condition is 5.17×10^7. In this paper, based on the calculation of 400 trains running every day, 16 cars are grouped into one group and a single car passes through one cycle, so the final lifespan of the discounted life is 22.14 years, meeting the standard service lifespan of 20–25 years.

4. Conclusion

At present, there is a lack of systematic and in-depth research on the failure mechanism of catenary components, but combined with the structural characteristics of the catenary and the analysis of operating conditions, it can be judged that the fretting damage and poor service environment are the main factors leading to the failure of catenary components.

(1) There are different situations of stress concentration at the key connection points of the catenary pillar, and the predicted fatigue lifespan of the key connection points of the pillar is around 22 years, which meets the design service life standards. The fatigue life of the cantilever structure is predicted to be about 12 years, which is much lower than the fatigue life of the catenary pillar as a whole. A complex environment during actual operation, long-term exposure to alternating loads and other factors together create good conditions for fretting damage.

(2) The fretting damage above the cantilever support is formed gradually, the process of which is long and not easy to be found, mainly manifesting in the surface coating peeling. Moreover, the mechanism of the fretting damage production is so complex that it is difficult to avoid.

(3) In order to avoid the protective coating peeling off and causing the pillar to be eroded by corrosive liquid for a long time, thus affecting its service life, it is necessary to check the coating condition of the root of the cantilever support of the catenary pillar regularly and paint new coating in time to protect the catenary pillar. The new technology of arc spraying ultra-fine sheet zinc aluminium coating has been successfully applied to contact wire supports and components, with significant corrosion resistance advantages, providing a better choice for surface corrosion prevention of contact wire-related components (Liu, 2023).

References

Cao, S., Ke, J., Deng, B., & Liu, X. (2010). The dynamic stability analysis of catenary system in strong wind area. *China Railway Science*, *31*(4), 79–84.

Chang, Z. (2013). Discussion on the application of contact network components for high-speed railway in low temperature and high wind area. *Safety and reliability technology of contact network components for high-speed railway*, 65–67.

Chen, G. Z. (2016). *Research on the Operation Performance of High-Speed Railway Contact Network*. MA thesis, Beijing: China Academy of Railway Sciences.

Cheng, D., Wen, Y. Q., Guo, Z. Q., Hu, X. Y., Wang, P. S., & Song, Z. K. (2024). Research on the evolution law of dynamic performance of CR400BF EMU train based on stochastic dynamics simulation. *Railway Sciences*, *3*(2), 143–155. doi: 10.1108/rs-01-2024-0004.

Diana, G., Bruni, S., Collina, A., & Fossati, F. (1998). High speed railways: Pantograph and overhead lines modelling and simulation. *WIT Transactions on The Built Environment*, *37*, 847–856.

Haiderali, A. E. (2020). Mitigation of ancient coal mining hazards to overhead line equipment structures. *Proceedings of the Institution of Civil Engineers – Transport*, *173*(4), 218–231. doi: 10.1680/jtran.18.00143.

Harak, S. S., Sharma, S. C., & Harsha, S. P. (2015). Modal analysis of prestressed draft pad of frei, ht wagons using finite element method. *Journal of Modern Transportation*, *23*(1), 43–49. doi: 10.1007/s40534-014-0064-9.

Jin, O., & Mall, S. (2004). Effects of slip on fretting behaviour: Experiments and analyses. *Wear*, *256* (7-8), 671–684. doi: 10.1016/s0043-1648(03)00510-6.

Li, K. (2017). *The analysis and structure optimization of cantilever structure and key components of overhead contact system based on ABAQUS*. Chengdu: Southwest Jiaotong University. MA thesis.

Link, M. (1981). Zur berechnung von fahrleitungsschwingungen mit hilfe frequenzabhängiger finiter elemente. *Ingenieur-Archiv*, *51*(1-2), 45–60. doi: 10.1007/bf00535954.

Link, M., & Nowak, B. (1987). Zur dynamischen Analyse des Systems Stromabnehmer und Fahrleitung, dargestellt am Beispiel des Intercity-Experimental. In *Proceedings of the Conference on Dynamik Fortschrittlicher Bahnsysteme* (pp. 245–262). VDI Berichte.

Liu, R. J. (2023). Research and prospect of surface corrosion protection technology for OCS parts. *Railway Construction Technology*, *45*(7), 43–45.

Liu, Z., Song, Y., & Liu, Y. (2015a). Aeolian vibration characteristics of electrified high-speed railway catenary. *Journal of Southwest Jiaotong University*, *50*(1), 1–6.

Liu, L., Yong, X. Y., & Guo, F.Y. (2015b). Research on the corrosion of metallic components of overhead contact system in typical atmospheric environment. *Journal of Railway Engineering Society*, *32*(3), 81–85.

Luo, J., Mo, J. L., Han, L. Q., Yan, J. F., & Zhang, Q. (2018a). Design on new cantilever and positioning device of overhead contact system of high-speed Railway. *Journal of the China Railway Society*, *40*(10), 36–42.

Luo, J., Lu, H. J., Yan, J. F., & Zhang, Q. (2018b). Research on the new support and positioning parts of catenary. *Journal of Railway Engineering Society*, *35*(12), 62–69.

Lykins, C. D., Mall, S., & Jain, V. (2001). A shear stress-based parameter for fretting fatigue crack initiation. *Fatigue and Fracture of Engineering Materials and Structures*, *24*(7), 461–473. doi: 10.1046/j.1460-2695.2001.00412.x.

Ministry of Railways, Department of Science and Technology (2009). *Provisional technical conditions for catenary equipment for OCS electrified railway*. Beijing: Ministry of Railways of the People's Republic of China.

Naidu, N., & Raman, S. G. S. (2005). Effect of shot blasting on plain fatigue and fretting fatigue behaviour of Al-Mg-Si alloy AA6061. *International Journal of Fatigue*, *27*(3), 323–331. doi: 10.1016/j.ijfatigue.2004.07.007.

Nakazawa, K., Sumita, M., & Maruyama, N. (1992). Effect of contact pressure on fretting fatigue of high strength steel and titanium alloy. *Standardization of fretting fatigue test methods and equipment*, 115–125. doi: 10.1520/stp25824s.

Poon, C., & Hoeppner, D. W. (1979). The effect of environment on the mechanism of fretting fatigue. *Wear*, *52*(1), 175–191. doi: 10.1016/0043-1648(79)90207-2.

Sakdirat, K., & Tao, T. (2019). Idealisations of synamic modelling for railway ballast in flood conditions. *Applied Science*, *9*(9), 1785.

Sakdirat, K., Chayut, N. H., & Lichen, R. (2021). Reliability quantification of railway electrification mast structure considering buckling. *Frontiers in Built Environment*, *7*, 1–10. doi: 10.3389/fbuil.2021.761491.

Tan, D. Q., Mao, J. L., Peng, J. F., Luo, J., Chen, W. R., & Zhu, M. H. (2018). Research and prospect on high-speed catenary component failure. *Journal of Southwest Jiaotong University*, *53*(3), 610–619.

Vinayag, A. T. (1983). Computer evaluation of controlled pantographs for current collection from simple catenary overhead equipment at high speed. *Journal of Dynamic Systems, Measurement, and Control*, *105*(4), 287–294. doi: 10.1115/1.3140673.

Vingsbo, O., & Söderberg, S. (1988). On fretting maps. *Wear*, *126*(2), 131–147. doi: 10.1016/0043-1648(88)90134-2.

Wang, G. (2009). Analysis and study of the deicing and anti-icing for catenary. *Journal of Railway Engineering Society*, *26*(8), 93–95.

Wang, Q. (2023). Study on the foundation of railway electrification catenary in permafrost region. *Journal of Railway Engineering Society*, *40*(12), 72–77.

Wang, Y., Deng, B., Li, H., Tian, Z., & Ke, J. (2005). The probability distribution law of the internal stress on each components of catenary system. *China Railway Science*, *26*(6), 45–47.

Wu, T. H. (1996). Analysis and calculation of catenary by FEM. *Journal of the China Railway Society*, 3, 44–49.

Xu, H. Y. (2014). Structural analysis and optimisation of deflection deformation of aluminium alloy cantilever for high-speed railway catenary. *China Railway*, 8, 54–58.

Xue, Q. W., & Du, X. Y. (2022). An improved fatigue life prediction model based on loading sequence. *Railway Sciences*, *1*(1), 90–97. doi: 10.1108/rs-04-2022-0015.

Xun, X., Yang, Y., Wang, Z., Gan, J., Wang, X. L., Gai, W. Y., & Li, Y. (2020). Three-dimensional fatigue crack propagation analysis and life prediction based on co-simulation of FRANC3D and ABAQUS. *Journal of Wuhan University of Technology*, *44*(3), 506–512.

Zhang, W. H., & Shen, Z. Y. (1991). Dynamic studies on catenary. *Journal of the China Railway Society*, 4, 26–33.

Zhang, Q., Li, X. F., Ma, Y. D., & Li, W. Q. (2023). Fatigue test loading method for wagon body based on measured load. *Railway Sciences*, *2*(1), 68–83. doi: 10.1108/rs-01-2023-0001.

Corresponding author
Wei Du can be contacted at: railwaydu@163.com

Zhongyu Yi, with a master's degree from Beijing University of Chemical Technology, is an assistant researcher and member of the Technical Committee on Steel Structure Anti-Corrosion Coating Systems under the National Technical Committee for Standardization of Coatings and Pigments. He mainly engages in research on steel structure corrosion and protection, as well as cleaning agents for engineering and machinery. He has participated in more than 20 railway industry projects and won 3 provincial and ministerial-level awards.